



## UV-photografting modification of NF membrane surface for NOM fouling reduction

M.N. Abu Seman<sup>a,\*</sup>, Nidal Hilal<sup>b</sup>, and M. Khayet<sup>c</sup>

<sup>a</sup>Faculty of Chemical and Natural Resources Engineering, Universiti Malaysia Pahang, Lebuhraya Tun Razak, 26300 Gambang, Kuantan, Pahang, Malaysia

Email: mazrul@ump.edu.my

<sup>b</sup>College of Engineering, Centre for Water Advanced Technologies and Environmental Research (C WATER), Swansea University, Swansea, SA2 8PP, UK

<sup>c</sup>Faculty of Physics, Department of Applied Physics I, University Complutense of Madrid, Av. Complutense s/n, Madrid 28040, Spain

Received 30 August 2012; Accepted 15 January 2013

---

### ABSTRACT

Fouling of natural organic matter is one of the common problems in water treatment plant. Despite physical and chemical treatment normally used to recover the flux loss, membrane surface properties also not less important to be considered. In this study, UV-photografting technique was applied to modify commercial nanofiltration (NF) membrane surface in order to reduce fouling tendency. Neutral hydrophilic N-vinylpyrrolidone has been chosen as the monomer for the UV-photografting. The result revealed that the grafted membrane at optimum conditions exhibits low humic acid fouling tendency compared with the unmodified membrane. In addition, both the unmodified and the UV-grafted polyethersulfone NF membranes were characterized in terms of structural properties (pore size,  $r_p$ , and ratio of membrane thickness to porosity,  $\Delta x/A_t$ ) using Pore Model in order to evaluate the effect of UV-photografting modification on structural parameters and indirectly influence the membrane performance and fouling as well.

*Keywords:* Nanofiltration; UV-photografting; Pore model; Fouling

---

### 1. Introduction

Membrane surface modification is extensively applied to increase membrane performance (i.e. high

permeate flux and rejection factor) and to reduce its fouling. Various methods have been considered such as interfacial polymerization [1,2], plasma treatment [3,4], ion beam [5], electron beam [6], chemical grafting polymerization [7,8], and UV-photografting polymerization

\*Corresponding author.

*Presented at the Conference on Membranes in Drinking and Industrial Water Production. Leeuwarden, The Netherlands, 10–12 September 2012.*

*Organized by the European Desalination Society and Wetsus Center for Sustainable Water Technology*

1944-3994/1944-3986 © 2013 The Authors. Published by Taylor & Francis.

This is an Open Access article. Non-commercial re-use, distribution, and reproduction in any medium, provided the original work is properly attributed, cited, and is not altered, transformed, or built upon in any way, is permitted. The moral rights of the named authors have been asserted.

[9–13]. Among these surface modification methods, UV-grafting has been widely used because of its simplicity, low cost, and breadth field of applications [14,15]. Some research studies show that surface modification by UV-grafting polymerization significantly affects the membrane morphology and its performance [16–18]. It was claimed that a successful membrane modification procedure should guarantee a reasonable permeate flux and a high rejection of the solutes under study without providing additional data to support their claims such as the membrane characteristics (i.e. membrane pore size and skin layer thickness) [8–12]. The permeate flux and rejection characteristics of the thin film composite nanofiltration (NF) membranes are normally determined by the morphology of the top thin layer supported by a microporous sublayer. The membrane pore size determines the selectivity, while the permeate flux depends on the thin layer thickness and pore density. Therefore, it is important to know the membrane pore size and the thin layer thickness not only its permeate flux and rejection factor.

There are several methods that can be used to estimate the membrane pore size: bubble point technique, mercury porosimetry, microscopic techniques (i.e. atomic force microscopy, AFM, and scanning electron microscopy, SEM), permporometry, thermoporometry, and solute transport method [19].

In this study, hydrodynamic model or pore model (PM) is applied to determine the pore size and the thickness of the membrane thin layer. The main objective is to characterize NF UV-grafted membranes by N-vinylpyrrolidone (NVP) in terms of physical properties and its effect on the membrane performance (i.e., permeability, rejection factor, and fouling index).

### 1.1. Characterization of NF membranes by PM

Generally, the solute separation or solute rejection is estimated as:

$$R = 1 - \frac{C_p}{C_b} \quad (1)$$

where  $C_p$  and  $C_b$  are the solute concentration in the permeate and in the bulk feed solutions, respectively. Due to the concentration polarization effect, the solute concentration at membrane surface is higher than in the bulk solution. Therefore, the real rejection factor is applicable to represent the membrane rejection as [20,21]:

$$R_{real} = 1 - \frac{C_p}{C_w} \quad (2)$$

where the membrane surface concentration,  $C_w$ , is not obtained directly from the experimental work. Based on the concentration polarization model,  $C_w$  can be correlated with the other measurable parameters (i.e. solute permeate flux,  $J_v$ , permeate concentration,  $C_p$ , and bulk concentration,  $C_b$ ) as [20,21]:

$$J_v = k \ln \frac{C_w - C_p}{C_b - C_p} \quad (3)$$

$k$  is the mass transfer coefficient in the boundary layer and can be determined from the following correlation [20,22]:

$$k = \frac{ShD_{i,\infty}}{d_H} \quad (4)$$

where  $D_{i,\infty}$  is the solute diffusion coefficient,  $d_H$  is the hydraulic channel diameter, and  $Sh$  is the Sherwood number.

### 1.2. Hydrodynamic model/PM

The most common approach used to model the transport of uncharged solute inside the membrane can be expressed by the hydrodynamic model or PM [23] as:

$$j_i = -D_{i,p} \frac{dc_i}{dx} + K_{i,c} c_i V \quad (5)$$

where  $j_i$  is the flux of solute  $i$  and the terms on the right hand side represents the transport due to diffusion and convection, respectively. Further details can be found elsewhere [23,24].

In order to obtain an expression for the rejection of the solute, Eq. (5) is integrated along the membrane thickness ( $0 < x < \Delta x$ ) with the solute concentrations in the membrane expressed in terms of the external concentration ( $C_w$  and  $C_p$ ) using the equilibrium partition coefficient,  $\Phi$ :

$$\Phi = \frac{c(0)}{C_w} = \frac{c(\Delta x)}{C_p} = (1 - \lambda)^2 \quad (6)$$

where  $\lambda = \frac{r_s}{r_p}$

Eq. (5) can be integrated and combined with Eq. (6) to give the following expression for the calculation of the real rejection factor:

$$R_{real} = 1 - \frac{C_p}{C_w} = 1 - \frac{K_{i,c} \Phi}{1 - \exp(-Pe_m)[1 - \Phi K_{i,c}]} \quad (7)$$

where the Peclet number,  $Pe_m$ , is defined as:

$$Pe_m = \frac{K_{i,c}}{K_{i,d}} \frac{V\Delta x}{D_{i,\infty} A_k} \quad (8)$$

According to Deen [25], the hindrance factors  $K_{i,c}$  and  $K_{i,d}$  are function of  $\lambda$  and are related to the hydrodynamic coefficients  $K^{-1}$ , the enhanced drag coefficient and the lag coefficient ( $G$ ) as follows:

$$K_{i,d} = K^{-1}(\lambda, 0) \quad (9)$$

$$K_{i,c} = (2 - \Phi)G(\lambda, 0) \quad (10)$$

These hydrodynamics coefficients with a limited range of  $\lambda$  ( $0 < \lambda < 0.95$ ) are well-expressed by Bowen and Mohammad [24] through third-order polynomial equations:

$$K^{-1}(\lambda, 0) = 1.0 - 2.401\lambda + 1.530\lambda^2 - 0.118\lambda^3 \quad (11)$$

$$G(\lambda, 0) = 1.0 + 0.042\lambda - 0.941\lambda^2 + 0.399\lambda^3 \quad (12)$$

In this model, the pure water flux is described by Hagen–Poiseuille equation, which relates the membrane structure parameters,  $r_p$  and  $\Delta x/A_k$  as:

$$J_w = \frac{r_p^2 \Delta P}{8\mu(\Delta x/A_k)} \quad (13)$$

where  $\Delta x$  is an effective membrane thickness and  $A_k$  is membrane porosity.

## 2. Experimental

### 2.1. Materials

The flat sheet membrane NFPE10 supplied by NADIR filtration GmbH (Germany) was used as support for UV-photografting polymerization technique. Its characteristics as specified by the manufacturer are summarized in Table 1. The neutral

Table 1  
Membrane characteristics provided by the manufacturer

Membrane	NFPE10
Material type	Hydrophilic
Pure water flux (l/m <sup>2</sup> h)	200–400
MWCO (Da)	1,000
NaCl rejection (0.5%)	10–20
Na <sub>2</sub> SO <sub>4</sub> rejection (1.0%)	40–70
Lactose retention (4.0%)	30–50
pH range	0–14
Maximum temperature (°C)	95

Table 2  
Characteristics of PEG solutes used in this study

Solutes	$D_{i,\infty} \times 10^{-10}$ (m <sup>2</sup> s <sup>-1</sup> )	$d_s$ (nm)
PEG200	7.18	0.64
PEG600	3.89	1.18
PEG1000	2.93	1.57
PEG3350	1.49	3.08

Table 3  
Summary of membrane modification parameters

Membrane	Monomer concentration (g/L)	Irradiation time (min)
NFPE10	–	–
<sup>a</sup> 5NVP-3 <sup>b</sup>	5	3
15NVP-1	15	1
30NVP-1	30	1
50NVP-1	50	1

<sup>a</sup>Concentration of monomer.

<sup>b</sup>Irradiation time.

monomer NVP, used for UV-photografting polymerization was purchased from Acros Organics Co. In this study, to determine the membrane pore size, polyethylene glycol (PEG) of different molecular weights in the range of 200 g/mol to 3,350 g/mol were chosen for NF membrane characterization. All PEG solutes were purchased by Sigma-Aldrich Co. The solute diameter and diffusivity of each PEG are shown in Table 2.

### 2.2. UV irradiation

UV-light system of wavelength 365 nm using a B-100 lamp (Ultra-Violet Products Ltd) with a radiation intensity of 21.7 mW/cm<sup>2</sup> was used to modify the membrane surface by immersion method. The UV-light intensity was measured by the light intensity meter (Cole Parmer Instrument Co., VLX-3W). The reactor system and the modification protocol were described previously (Abu Seman et al., 2012). The membrane was modified using different concentration of monomers for a predetermined irradiation time. Table 3 shows the summary of the membrane modification conditions.

### 2.3. Membrane characterization

#### 2.3.1. Membrane permeability and natural organic matter fouling

NF experiments have been carried out using a plate-and-frame membrane module with an effective

area of 12.6 cm<sup>2</sup>, which can be operated under a transmembrane pressure in the range of 100–900 kPa. For each membrane, three samples were considered and the results were averaged. The feed solution is circulated through the membrane module by a pressure pump (D series, Tuthill Pump Co., California). In all NF experiments, the feed and retentate flow rates were maintained at 0.4 L/min. The permeate flux ( $J$ ) of each membrane sample was determined by weighing the obtained permeate during a predetermined time using an electronic balance (Precisa, Model XB3200C) connected to a computer and calculated by the following equation.

$$J = \frac{W}{A\Delta t} \quad (14)$$

where  $W$  is the weight of the obtained permeate during a predetermined NF operation time ( $\Delta t$ ) and  $A$  is the membrane area.

Before all NF experiments, each membrane was pressurized at 700 kPa for at least 2 h using deionized water to reduce compaction effect. Subsequently, the pure water experiments were conducted at different transmembrane pressures,  $\Delta P$  (400, 500, 600 and 700 kPa) in order to determine the pure water permeation flux ( $J_w$ ) using Eq. (14). The membrane permeability,  $P_m$ , was determined from the slope of the straight line that can be obtained by plotting the permeate flux ( $J_w$ ) against  $\Delta P$  following the following equation.

$$P_m = \frac{J_w}{\Delta P} \quad (15)$$

Humic acid (Sigma Aldrich) aqueous solutions were used as a NOM model and tested at transmembrane pressure of 600 kPa. In this study, the pH of humic acid feed solution with a concentration of 15 mg/L was adjusted at pH 7 and pH 3 by using 0.1 M NaOH or 0.1 M HCl. For both the un-grafted and the UV-grafted membranes, before and after NF experiments with humic acid solution, the system was washed with deionized water and the pure water permeation flux ( $J_{wf}$ ) was measured again in order to evaluate the irreversible fouling in terms of pure water flux reduction, called hereafter irreversible fouling factor ( $FR_w$ ). This is determined as follows [26,27].

$$FR_w = \frac{J_{w0} - J_{wf}}{J_{w0}} \times 100 \quad (16)$$

### 2.3.2. Determination of structural parameters

In order to estimate membrane pore radius ( $r_p$ ), NF experiments were conducted using aqueous solutions containing PEG solute with a concentration of 200 ppm, a feed operating pressure of 600 kPa and a feed flow rate of 0.4 L/min. The feed solution temperature was maintained constant at room temperature. The solute concentration in the feed, retentate, and permeate were measured by the total organic carbon analyzer and solute rejection ( $R$ ) was calculated using Eq. (1).

### 2.3.3. AFM analysis

The surface of both the un-grafted and the grafted membranes were characterized by a multimode AFM (Veeco Instruments (USA)). Comprehensive reviews on membrane characterization by AFM are available in the literature [28,29]. The images were obtained over different areas of each membrane sample. In this study, tapping mode was used, and the same tip was employed to scan the surface of all membranes. Finally, all captured images were treated in the same way. From the obtained AFM images, the root mean square roughness, RMS, was determined considering the same scan range of 5  $\mu\text{m} \times 5 \mu\text{m}$  for all images.

## 3. Results and discussions

### 3.1. Membrane water permeation

The water permeation of each membrane was determined from the measurements of the water flux as a function of the applied pressure. The obtained pure water permeability ( $P_m$ ) of the un-grafted and the UV-grafted membranes are summarized in Table 4. The permeability of the NVP UV-grafted membranes was found to be lower than that of the unmodified NFPE10. In our previous study [18], this phenomenon was discussed in terms of monomer hydrophilicity, monomer reactivity and monomer size based on other research findings without considering the mem-

Table 4  
Membrane permeability of the un-grafted NFPE10 membrane and NVP UV-grafted membranes

Membrane	Water permeability, $P_m$ (m <sup>3</sup> /m <sup>2</sup> s Pa) $\times 10^{-11}$
Un-grafted	4.32
5NVP-3	3.46
15NVP-1	3.70
30NVP-1	3.16
50NVP-1	2.86

brane structure parameters. In order to understand this phenomenon, the PM was considered to determine the membrane structure properties (i.e.  $r_p$  &  $\Delta x/A_k$ ) and its effect on the membrane performance.

### 3.2. Membrane characterization using PM

Based on PM, the membrane pore radius ( $r_p$ ) can be determined by solving Eq. (7). The results are given in Table 5 for the membrane NFPE10 and the UV-grafted membranes. It was observed that different pore radius was obtained from different individual PEG solutes. For example, the obtained pore radius of the membrane NFPE10 using PEG200 is 0.58 nm; however, it is 1.62 nm when the PEG molecular weight is higher (PEG3350). It seems that when the molecular weight of the used solute is higher the

obtained membrane pore size is larger. The variation of  $r_p$  values represented by the individual PEG solutes indicates that the membrane possess a wide range of pore size. An average value (i.e. mean) and the corresponding standard deviation were calculated and the obtained results are also shown in Table 5. For all membranes, the  $r_p$  value calculated using PEG3350 was excluded from the calculation of the average value due to the limitation of value. It was observed that for all membranes, the  $\lambda$  value given by PEG3350 is more than 0.95, which is not valid for PM ( $0 < \lambda < 0.95$ ). This phenomenon could be explained by the membrane MWCO as well. For example, in the case of NFPE10 membrane with a MWCO of 1,000 Da (as provided by manufacturer), any solute with a molecular weight higher than this value is not preferable for membrane characterization since the

Table 5  
Structure parameters obtained from PM model of the un-grafted NFPE10 and NVP UV-grafted membranes

Membrane	Solutes	$R_{real}$ (%)	$(\lambda = r_s/r_p)$	$r_p$ (nm)	$\Delta x/A_k$ ( $\mu\text{m}$ ) <sup>a</sup>
Un-grafted	PEG200	40.04	0.552	0.58	1.02
	PEG600	84.55	0.670	0.88	2.36
	PEG1000	95.74	0.809	0.97	2.87
	PEG3350	99.78	0.951	1.62 <sup>b</sup>	–
	Average			0.81 ± 0.20	2.08 ± 0.96
5NVP-3	PEG200	26.90	0.451	0.71	1.92
	PEG600	88.14	0.702	0.84	2.69
	PEG1000	96.09	0.818	0.96	3.51
	PEG3350	99.84	0.963	1.60 <sup>b</sup>	–
	Average			0.84 ± 0.13	2.71 ± 0.80
15NVP-1	PEG200	27.10	0.457	0.70	1.74
	PEG600	86.19	0.686	0.86	2.63
	PEG1000	95.67	0.818	0.96	3.28
	PEG3350	99.88	0.969	1.59 <sup>b</sup>	–
	Average			0.84 ± 0.13	2.55 ± 0.77
30NVP-1	PEG200	18.22	0.368	0.87	3.15
	PEG600	88.93	0.711	0.83	2.87
	PEG1000	96.91	0.835	0.94	3.68
	PEG3350	99.89	0.969	1.59 <sup>b</sup>	–
	Average			0.88 ± 0.06	3.23 ± 0.41
50NVP-1	PEG200	25.93	0.451	0.71	2.32
	PEG600	92.33	0.756	0.78	2.80
	PEG1000	98.05	0.872	0.90	3.73
	PEG3350	99.91	0.975	1.58 <sup>b</sup>	–
	Average			0.80 ± 0.10	2.95 ± 0.72

<sup>a</sup>Calculated based on Hagen–Poiseuille (Eq. (13)).

<sup>b</sup>These data were excluded from the average value of  $r_p$  due to the limitation of  $\lambda$  value ( $0 < \lambda < 0.95$ ).

solute radius ( $r_s$ ) is bigger than the pore radius ( $r_p$ ) and almost all the solutes are rejected. In order to keep the value of  $\lambda = r_s/r_p$  less than 0.95 to maintain the validation of the PM model, the  $r_s$  value must be always less than  $r_p$  ( $r_s < r_p$ ). However, in the case of PEG3350, where the solute radius is almost similar or greater than the pore radius ( $r_s \geq r_p$ ), the obtained  $\lambda$  values are deviated from the limitation.

As can be seen from Table 5, all membranes exhibit pore radius in the range of NF membranes. Based on the PM model, with exception of the membranes modified using the highest monomer concentration (50NVP-1), the NVP UV-grafted membranes exhibit slightly larger pores size than the un-grafted membrane NFPE10. In terms of water permeability, the NVP UV-grafted membranes exhibited lower values than the un-grafted NFPE10 membrane (Table 4), although the NVP UV-grafted membranes possess larger pore sizes. This may be due to the thickness of the formed grafted polymer layer. Using the average  $r_p$  values given by the PM model, another important parameter, ratio of the membrane thickness and porosity ( $\Delta x/A_k$ ) was determined using Eq. (13). The results are summarized in Table 5. The NVP UV-grafted membranes show a higher value of  $\Delta x/A_k$  compared with the un-grafted membrane NFPE10. The results show that NVP UV-grafting modification produced a thicker membrane top layer that contributes to the increase in the membrane resistance (i.e. decrease in the membrane permeability compared with the un-grafted NFPE10 membrane), although the pore size of the NVP UV-grafted membranes are greater. This result clarified our previous speculation [18] that the neutral NVP monomer grafted on the membrane surface produced a thicker layer than the un-grafted NFPE10 membrane. In general, even there is a slight change in pore size was observed after modification, this changes, however, is not too significant compared with the other structure parameter ( $\Delta x/A_k$ ). As can be seen in Fig. 1, regardless of irradiation

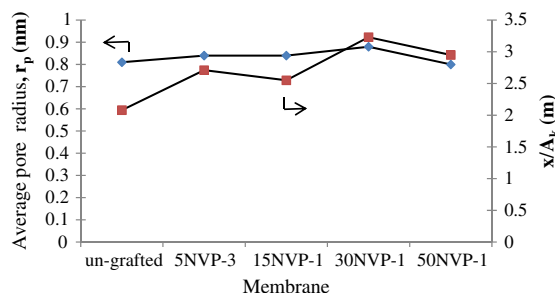


Fig. 1. Comparison of the average pore size,  $r_p$  and  $\Delta x/A_k$  of the un-grafted NFPE10 and the NVP UV-grafted membranes obtained from PM.

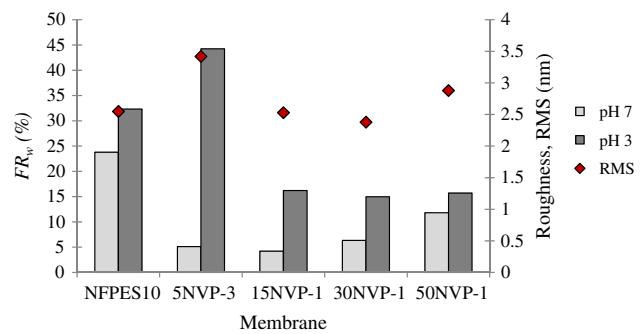


Fig. 2. Correlation between membrane roughness, (RMS) and irreversible fouling factor, ( $FR_w$ ) of un-grafted NFPE10 and UV-grafted membranes at different pH environment.

tion time, the ratio of membrane thickness to porosity ( $\Delta x/A_k$ ) increased as the NVP monomer was increased.

### 3.3. NOM fouling

The results of the NOM irreversible fouling factor,  $FR_w$ , of the un-grafted and the UV-grafted membranes by NVP are shown in Fig. 2 using humic acid aqueous solutions of pH 7 and 3, respectively. At neutral pH, all UV-grafted membranes exhibited a lower irreversible fouling factor than that of the un-grafted membrane. This may attributed by the existence of a new thicker grafted hydrophilic PVP layer on the membrane reduce the interaction between humic acid molecules and membrane surface, hence reduce fouling. Moreover, for all membranes, it can be observed that the irreversible fouling at a pH 7 is less than that at pH3. This result is influenced by the change of the humic acid characteristics at different pH environments [30]. When humic acid molecules become coiled, spherical in shape and compact at pH 3, the effect of roughness on fouling is more significant than at pH7. As can be seen clearly in Fig. 2, even 5NVP-3 membrane has higher thickness (correspond to thicker hydrophilic PVP layer) than un-grafted NFPE10 membrane, it still exhibits the highest  $FR_w$  value at pH 3 and this may due to the highest value of roughness as indicated by RMS. This means that at pH3, the membrane hydrophilicity becomes less important but the surface morphology (i.e. roughness in this study) more significant effects on the membrane fouling.

## 4. Conclusions

The commercial NF NFPE10 membrane was successfully modified by UV-photografting polymerization method using the neutral hydrophilic monomer

NVP. The result reveals that UV-grafting significantly affects the membrane structure parameter (pore size and skin layer thickness) and consequently the membrane performance. The obtained pore size values of all membranes are in the range of commercial NF membrane characteristics [24]. In terms of membrane thin layer thickness, membranes grafted with NVP are thicker than the un-grafted NFPE10. NOM-fouling experiment showed that the grafted NVP membranes exhibited high antifouling characteristics than un-grafted one at neutral pH environment. However, under acidic condition of pH3, membrane roughness significantly affects the membrane fouling than hydrophilicity characteristic.

In general, it can be concluded that under both pH environments (neutral and acidic), a moderate NVP concentration (15 g/L in our study) is enough to produce a good membrane with lower fouling.

## References

- [1] M.N. Abu Seman, M. Khayet, N. Hilal, Development of antifouling properties and performance of nanofiltration membranes modified by interfacial polymerisation, *Desalination* 273 (2011) 36–47.
- [2] M.N. Abu Seman, M. Khayet, N. Hilal, Nanofiltration thin-film composite polyester polyethersulfone-based membranes prepared by interfacial polymerization, *J. Membr. Sci.* 348 (2010) 109–116.
- [3] H. Chen, G. Belfort, Surface modification of poly(ether sulfone) ultrafiltration membranes by low-temperature plasma-induced graft polymerization, *J. Appl. Polym. Sci.* 72 (1999) 1699–1711.
- [4] M. Ulbricht, G. Belfort, Surface modification of ultrafiltration membranes by low temperature plasma II. Graft polymerization onto polyacrylonitrile and polysulfone, *J. Membr. Sci.* 111 (1996) 193–215.
- [5] R. Chennamsetty, I. Escobar, Evolution of polysulfone nanofiltration membrane following ion beam irradiation, *Langmuir* 24 (2008) 5569–5579.
- [6] A. Linggawati, A.W. Mohammad, Z. Ghazali, Effect of electron beam irradiation on morphology and sieving characteristics of nylon-66 membranes, *Eur. Polym. J.* 45 (2009) 2797–2804.
- [7] V. Freger, J. Gilron, S. Belfer, TFC polyamide membranes modified by grafting of hydrophilic polymers: An FT-IR/AFM/TEM study, *J. Membr. Sci.* 209 (2002) 283–292.
- [8] T. Carroll, N.A. Booker, J. Meier-Haack, Polyelectrolyte-grafted microfiltration membranes to control fouling by natural organic matter in drinking water, *J. Membr. Sci.* 203 (2002) 3–13.
- [9] H. Susanto, H. Arafat, E.M.L. Janssen, M. Ulbricht, Ultrafiltration of polysaccharide-protein mixtures: Elucidation of fouling mechanisms and fouling control by membrane surface modification, *Sep. Purif. Technol.* 63 (2008) 558–565.
- [10] A.H.M. Yusof, M. Ulbricht, Polypropylene-based membrane adsorbers via photo-initiated graft copolymerization: Optimizing separation performance by preparation conditions, *J. Membr. Sci.* 311 (2008) 294–305.
- [11] M. Taniguchi, G. Belfort, Low protein fouling synthetic membranes by UV-assisted surface grafting modification: Varying monomer type, *J. Membr. Sci.* 231 (2004) 147–157.
- [12] J. Pieracci, D.W. Wood, J.V. Crivello, G. Belfort, Increasing membrane permeability of UV-modified poly(ether sulfone) ultrafiltration membranes, *J. Membr. Sci.* 202 (2002) 1–16.
- [13] V. Kochkodan, N. Hilal, V. Melnik, Selective recognition of organic pollutants in aqueous solutions with composite imprinted membranes, *Adv. Colloid Interface Sci.* 159 (2010) 180–188.
- [14] N. Hilal, L. Al-Khatib, B.P. Atkin, V. Kochkodan, N. Potapchenko, Photochemical modification of membrane surfaces for (bio)fouling reduction: A nano-scale study using AFM, *Desalination* 158 (2003) 65–72.
- [15] Y. Uyama, K. Kato, Y. Ikada, Surface modification of polymers by grafting, *Adv. Polym. Sci.* 137 (1998) 1–39.
- [16] M. Khayet, M.N. Abu Seman, N. Hilal, Response surface modeling and optimization of composite nanofiltration modified membranes, *J. Membr. Sci.* 349 (2010) 113–122.
- [17] M.N. Abu Seman, M. Khayet, Z.I. Bin Ali, N. Hilal, Reduction of nanofiltration membrane fouling by UV-initiated graft polymerization technique, *J. Membr. Sci.* 355 (2011) 133–141.
- [18] M.N. Abu Seman, M. Khayet, N. Hilal, Comparison of two different UV-grafted nanofiltration membranes prepared for reduction of humic acid fouling using acrylic acid and N-vinylpyrrolidone, *Desalination* 287 (2012) 19–29.
- [19] M. Mulder, *Basic Principles of Membrane Technology*, second ed., Kluwer Academic, Dordrecht, 2000.
- [20] K.Y. Wang, T.S. Chung, The characterization of flat composite nanofiltration membranes and their applications in the separation of Cephalexin, *J. Membr. Sci.* 247 (2005) 37–50.
- [21] W.R. Bowen, S.Y. Cheng, T.A. Doneva, D.L. Oatley, Manufacture and characterisation of polyetherimide/sulfonated poly(ether ether ketone) blend membranes, *J. Membr. Sci.* 250 (2005) 1–10.
- [22] Schaep, J. Nanofiltration for the removal of ionic components from water. PhD Thesis. Belgium: Katholieke Universiteit Leuven; (1999).
- [23] Y. Kiso, K. Muroshige, T. Oguchi, T. Yamada, M. Hhirose, T. Ohara, T. Shintani, Effect of molecular shape on rejection of uncharged organic compounds by nanofiltration membranes and on calculated pore radii, *J. Membr. Sci.* 358 (2010) 101–113.
- [24] W.R. Bowen, A.W. Mohammad, Characterization and prediction of nanofiltration membrane performance- A general assessment. *I. Chem. E.* 76 Part A (1998) 885–893.
- [25] W.M. Deen, Hindered transport of large molecules in liquid filled pores, *AIChE J.* 33 (1987) 1409–1425.
- [26] M. Mänttäri, L. Puro, J. Nuortila-Jokinen, M. Nyström, Fouling effects of polysaccharides and humic acid in nanofiltration, *J. Membr. Sci.* 165 (2000) 1–17.
- [27] M. Mänttäri, M. Nyström, Critical flux in NF of high molar mass polysaccharides and effluents from the paper industry, *J. Membr. Sci.* 170 (2000) 257–273.
- [28] N. Hilal, W.R. Bowen, L. Alkhatib, O. Ogunbiyi, A review of atomic microscopy applied to cell interactions with membrane, *Trans. IChemE A Chem. Eng. Res. Des.* 84 (A4) (2006) 282–292.
- [29] W.R. Bowen, N. Hilal, R.W. Lovitt, C.J. Wright, Characterisation of membrane surfaces: Direct measurement of biological adhesion using an atomic force microscope, *J. Membr. Sci.* 154 (1999) 205–212.
- [30] S. Hong, M. Elimelech, Chemical and physical aspects of natural organic matter (NOM) fouling of nanofiltration membranes, *J. Membr. Sci.* 132 (1997) 159–181.